A New Model for Multi-objective Load Curtailment Applied on Deregulated Environment

SIGE LIU, XIAOXIN ZHOU, MINGTIAN FAN, HAOZHONG CHENG
Department of Electrical Engineering
Shanghai Jiaotong University
Dongchuan Road 800, Minhang District, Shanghai, 200240
P R CHINA
sgliu@epri.ac.cn; lsgluke@126.com

Abstract: - In the deregulated environment, transmission congestion is one major problem that needs to be handled in power system operation. This paper aims to alleviate congestion using the multi-objective load curtailment (MOLC) approach. The proposed MOLC approach optimizes the two objectives simultaneous, namely the security margin and load curtailment cost. The security margin is measured by a presented voltage instability indictor (VSI). A fitting coefficient is adopted to combine the two conflicted objectives. The primal dual interior point method (PDIPM) is adopted to solve the proposed MOLC model. The effectiveness of both the improved PDIPM and the MOLC approach has been tested and proven on the modified IEEE 30-bus system and IEEE 118-bus system. The results obtained show that the proposed technique is able to improve system security while yielding lower cost of load curtailment.
Key-Words: - Multi-objective load curtailment, voltage instability indicator, security margin, cost of load curtailment, fitting coefficient, primal dual interior point method

1 Introduction

The restructuring and deregulation of the power industry has significantly changed the function of the power system resulting in significant competitive, technological and regulatory changes [1]. Congestion management [2] has been proposed to deal with the increased demand and competition. The congestion may be caused by a contingency, loss of generation or requirements for secure operation of the transmission network. It is crucial for a competitive power market to have the transmission congestion alleviated and controlled. To alleviate congestion in the network system, one possible solution is to adjust or curtail load.

Load curtailment programs are functional in various markets across the world. In some countries, availability of load curtailment is viewed as an ancillary service [3]. In ref. [4-8], some rules for the load curtailment are proposed and discussed.

The process of curtailing load by the system dispatcher is an optimal system dispatch problem, which is the focus of this paper, looks at the specified optimal load curtailment scheme to have the transmission congestion alleviated.

In the field of load curtailment problem, single objective load curtailment models have been adopted and cost of load curtailment has been proposed to describe the curtail degree. Compared with single objective load curtailment approach, the multi-objective load curtailment (MOLC) in a deregulated environment is an appropriate way to handle several objectives simultaneously and also an efficient way to harmonize the usually conflicting objectives. Taking the security margin into account in the MOLC model is a valuable research topic which so far has not been considered and studied seriously.

From the viewpoint of the overall system, this paper presents a MOLC model, which aims to improve the security margin and to alleviate cost of load curtailment simultaneous during contingency states. A security margin index namely voltage instability indicator is presented to measure the security degree and it is set as one of optimization objectives in the proposed mathematic model of MOLC. A fitting coefficient is presented to combine the two conflicting objectives into one equivalent objective. An effective primal dual interior point method (PDIPM) is adopted to solve the proposed MOLC model.

This paper is organized as fellows: In Section 2, the voltage instability indicator is proposed to describe the security margin. In Section 3, the MOLC model is presented. In Section 4, the PDIPM and its application in the MOLC are presented. In Section 5, case studies carried out on both a modified IEEE-30 bus system and an IEEE-118 bus system. Finally, the conclusions drawn from the study is provided in Section 6.

2 Security Margin Index

In this section, to analyze the voltage security of system, a voltage instability indicator is presented to describe the voltage security degree.

Voltage instability indicator at any bus i, based on the maximum power transfer theorem can be defined as [9, 10]:

$$VSI_i = \frac{Z_{ii}^{\text{Bus}}}{Z_i^{\text{Load}}} = \frac{Z_{ii}^{\text{Bus}}}{V_{Li}^2 \cos\phi_i} P_{Li} \tag{1}$$

$$Z_i^{\text{Load}} = \frac{V_{Li}^2}{S_i} = \frac{V_{Li}^2}{P_{Li} / \cos\phi_i} = \frac{V_{Li}^2}{P_{Li}} \cos\phi_i \tag{2}$$

Lower the instability indicator more is the security margin. Therefore, maximizing the security margin would entail minimizing the (maximum) instability index. As *VSI* tends to unity, the system tends to reach its load ability limit.

The base case load at bus i is as follow:

$$S_{Li} = P_{Li} + jQ_{Li} \tag{3}$$

The post-dispatch load at bus i is as follows:

$$S_{Li}^{'} = S_{Li} + \Delta S_{Li} = (P_{Li} - P_{ci}) + j(Q_{Li} - Q_{ci}) \tag{4}$$

Q_{ci} is computed from P_{ci} and ϕ_i (in this paper, ϕ_i is assumed as a constant).

Therefore, the load impedance at bus i after dispatching an additional load ΔS_{Li} is defined as:

$$Z_i^{'\text{Load}} = \frac{V_{Li}^{'\,2}}{S_{Li}^{'}} = \frac{V_{Li}^{'\,2} \cos\phi_i}{P_{Li}^{'}} = \frac{V_{Li}^{'\,2} \cos\phi_i}{P_{Li} - P_{ci}} \tag{5}$$

Here, $V_{Li}^{'} = V_{Li}^{0} + \Delta V_{Li}$, V_{Li}^{0} and $V_{Li}^{'}$ are the pre-dispatch voltage and post-dispatch voltages of bus i, respectively. Therefore, the post-dispatch instability indicator is defined as:

$$VSI_i^{'} = \frac{Z_{ii}^{\text{Bus}}}{Z_i^{'\text{Load}}} = \frac{Z_{ii}^{\text{Bus}}}{V_{Li}^{'2} \cos\phi_i} P_{Li}^{'} = b_i (P_{Li} - P_{ci}) \tag{6}$$

$$b_i = \frac{Z_{ii}^{\text{Bus}}}{V_{Li}^{'2} \cos\phi_i} \tag{7}$$

Due to the dependence of the state variables $\boldsymbol{V}$ on the variables $\boldsymbol{P}_c$, it is envisaged that an iterative solution would be necessary. In enq.6, the bus voltage would be calculated and updated for the particular decrease in the load. So although V_{Li} is a variable quantity (a function of the decision variable), it would be constant (while optimizing) for a particular value of load during a particular iteration in the iterative process. So b_i is a constant.

Denoting $\lambda = \max\{VSI_i(\cdot)\}$, $i \in NC$, λ represents the security margin of the system. In this paper, λ also be formulated as follow:

$$\lambda = \max\{VSI_i(\boldsymbol{P}_c)\},\ i \in NC \tag{8}$$

The security margin index λ can quantitatively describe the level of system voltage security in a synthetic way. In this paper, it will be taken as a key objective in the MOLC model.

3 Mathematic Model of MOLC

Using the security margin index and cost function of load curtailment, a MOLC model is designed to implement the load curtailment in system operation. The specified MOLC mathematic model based on the AC power flow is presented in this section.

In this paper, the primary aim of load curtailment would be safeguard the system security. At same time, it would be beneficial to minimize the "cost" incurred in the curtailment. Two objectives are included in MOLC problem, which are security margin and cost incurred for load curtailment. Maximizing the security margin $f_1(S)$ and minimizing the cost incurred for load curtailment $f_2(S)$, simultaneously, could be two conflicting objectives. $f_1(S)$ and $f_2(S)$ are described below for a given scenario S.

Minimization of security margin index λ, which represents the security margin of the system from the point of view of voltage stability.

$$f_1(S) = \lambda \tag{9}$$

Minimization of the cost incurred for load curtailment.

$$f_2(S) = \sum_{i \in NC} k_i P_{ci} \tag{10}$$

To combine the two objectives, it has defined a multi-objective function f.

$$f = \omega_1 f_1 + \omega_2 f_2 \tag{11}$$

The constraints of OLC problem include equality and inequality constraints.

Subject to equality constraints $\boldsymbol{g}(\cdot)$:

$$\begin{cases} P_i(\boldsymbol{V},\boldsymbol{\theta}) + (P_{Li} - P_{ci}) - P_{Gi} = 0 & i \in N \\ Q_i(\boldsymbol{V},\boldsymbol{\theta}) + (Q_{Li} - Q_{ci}) - Q_{Gi} = 0 & i \in N \\ P_{ci} / P_{Li} = Q_{ci} / Q_{Li} & i \in NC \end{cases} \tag{12}$$

Subject to inequality constraints $\boldsymbol{h}(\cdot)$:

$$\begin{cases} 0 \le P_{ci} \le P_{ci}^{\max} & i \in NC \\ P_{Gi}^{\min} \le P_{Gi} \le P_{Gi}^{\max} & i \in NG \\ Q_{Gi}^{\min} \le Q_{Gi} \le Q_{Gi}^{\max} & i \in NG \\ T_l(\boldsymbol{V},\boldsymbol{\theta}) \le T_l^{\max} & l \in L \\ V_i^{\min} \le V_i \le V_i^{\max} & i \in N \end{cases} \tag{13}$$

$\boldsymbol{x} = [\boldsymbol{P}_C^{\text{T}}\ \boldsymbol{P}_G^{\text{T}}\ \boldsymbol{Q}_G^{\text{T}}\ \boldsymbol{V}^{\text{T}} \boldsymbol{\theta}^{\text{T}}]^{\text{T}}$ is the vector of decision variables including the vector of state variables ($\boldsymbol{V}$ and $\boldsymbol{\theta}^{\text{T}}$) and vector of control variables ($\boldsymbol{P}_G^{\text{T}}$, $\boldsymbol{Q}_G^{\text{T}}$

and $\boldsymbol{P}_C^{\mathrm{T}}$). The model of MOLC problem (9)-(13) can be formulated as follows:

$$\begin{cases} \min & f(\boldsymbol{x}) \\ \text{s.t.} & \boldsymbol{g}(\boldsymbol{x}) = 0 \\ & \boldsymbol{h}^{\min} \le \boldsymbol{h}(\boldsymbol{x}) \le \boldsymbol{h}^{\max} \end{cases} \tag{14}$$

In the multi-objective function *f*, two terms are presented, with their influence on the final solution being determined by the value of the weighting factors ω_1 and ω_2. The first certain guarantees the security margin, whereas the second term presents the cost of load curtailment. Observe that $\omega_1 > 0$, since for $\omega_2 = 0$ there would be no representation of the market in the proposed MOLC formulation, rendering it useless. Notice that the two terms of the objective function are expressed in different units, since the cost of load curtailment affect the chosen values of ω_1 and ω_2 (typically, $\omega_1 << \omega_2$). However, it is possible to assume that $\omega_1 = \omega$ and $\omega_2 = 1-\omega$, with proper scaled valued of ω for each system under study ($0<\omega<1$), as this simplifies the optimization problem without losing generality.

4 The PDIPM Algorithm

In eqn.14, the MOLC model involves nonlinear objectives and constraint functions so it can be regarded as a nonlinear optimization problem. Many proposed optimization methods can be used to solve this nonlinear optimization problem. Among the many variants of optimization methods, IPM has become an efficient solution algorithm due to its theoretical complexity properties and computational efficiency [11-16]. In this section, a PDIPM is presented in detail.

4.1 The PDIPM

The MOLC problem can be solved by an IPM based on a logarithmic barrier primal-dual algorithm defined in [5] and [6]. In this method, are first assumed to be continuous. Besides the slack variables, the Largrane multipliers are introduce

First of all, by introducing slack variable vectors $(\boldsymbol{y},\boldsymbol{z}) \in R^m$ eqn.14 is transformed to eqn.15.

$$\begin{cases} \min & f(\boldsymbol{x}) \\ \text{s.t.} & \boldsymbol{g}(\boldsymbol{x}) = 0 \\ & \boldsymbol{h}(\boldsymbol{x}) - \boldsymbol{y} - \boldsymbol{h}^{\min} = 0 \\ & \boldsymbol{h}(\boldsymbol{x}) + \boldsymbol{z} - \boldsymbol{h}^{\max} = 0 \\ & \boldsymbol{y} \ge 0, \quad \boldsymbol{z} \ge 0 \end{cases} \tag{15}$$

The slack variables vectors $\boldsymbol{y}$ and $\boldsymbol{z}$ are transformed to logarithmic barrier functions and are incorporated into the objective function of eqn.15. So enq.15 is transformed to eqn.16.

$$\begin{cases} \min & f(\boldsymbol{x}) - \mu^k \sum_{i=1}^{m} (\ln y_i + \ln z_i) \\ \text{s.t.} & \boldsymbol{g}(\boldsymbol{x}) = 0 \\ & \boldsymbol{h}(\boldsymbol{x}) - \boldsymbol{y} - \boldsymbol{h}^{\min} = 0 \\ & \boldsymbol{h}(\boldsymbol{x}) + \boldsymbol{z} - \boldsymbol{h}^{\max} = 0 \\ & \boldsymbol{y} \ge 0 \quad \boldsymbol{z} \ge 0 \end{cases} \tag{16}$$

In eqn.16, μ^k is represented barrier factor and k is represented kth iteration. Eqn.16 is formulated as an optimal problem with equality constraints that can be transformed to a Lagrangian function showed as eqn.17.

$$\begin{aligned} L_\mu(\boldsymbol{w}) = {} & f(\boldsymbol{x}) - \mu^k \sum_{i=1}^{m} (\ln y_i + \ln z_i) - \boldsymbol{\lambda}^{\mathrm{T}} \boldsymbol{g}(\boldsymbol{x}) \\ & - \boldsymbol{\gamma}^{\mathrm{T}} (\boldsymbol{h}(\boldsymbol{x}) - \boldsymbol{y} - \boldsymbol{h}^{\min}) + \boldsymbol{\pi}^{\mathrm{T}} (\boldsymbol{h}(\boldsymbol{x}) + \boldsymbol{z} - \boldsymbol{h}^{\max}) \end{aligned} \tag{17}$$

Where $\boldsymbol{w} = \{\boldsymbol{x},\boldsymbol{y},\boldsymbol{z},\boldsymbol{\lambda},\boldsymbol{\gamma},\boldsymbol{\pi}\}$; variable vector $\boldsymbol{x}$, $\boldsymbol{y}$ and $\boldsymbol{z}$ are defined as dual variable; variable vector $\boldsymbol{\lambda}$, $\boldsymbol{\gamma}$ and $\boldsymbol{\pi}$ are defined as primal variable. Where $\boldsymbol{x} \in R^n$, $\boldsymbol{\lambda} \in R^n$, $\boldsymbol{y} \in R^m$, $\boldsymbol{z} \in R^m$, $\boldsymbol{\gamma} \in R^m$, $\boldsymbol{\pi} \in R^m$.

According to KKT condition, when the gradient of Lagrangian function equals to zero it can reach its local minimum. That is shown as eqn.18.

$$\frac{\partial L_\mu}{\partial \boldsymbol{w}} = \begin{bmatrix} \left[\frac{\partial f}{\partial \boldsymbol{x}}\right] - \left[\frac{\partial \boldsymbol{g}}{\partial \boldsymbol{x}}\right]^{\mathrm{T}} \boldsymbol{\lambda} - \left[\frac{\partial \boldsymbol{h}}{\partial \boldsymbol{x}}\right]^{\mathrm{T}} \boldsymbol{\gamma} + \left[\frac{\partial \boldsymbol{h}}{\partial \boldsymbol{x}}\right]^{\mathrm{T}} \boldsymbol{\pi} \\ \boldsymbol{Y\gamma} - \mu^k \boldsymbol{u} \\ \boldsymbol{Z\pi} - \mu^k \boldsymbol{u} \\ -g(\boldsymbol{x}) \\ -\boldsymbol{h}(\boldsymbol{x}) + \boldsymbol{y} + \boldsymbol{h}^{\min} \\ \boldsymbol{h}(\boldsymbol{x}) + \boldsymbol{z} - \boldsymbol{h}^{\max} \end{bmatrix} = [0] \tag{18}$$

Where $\boldsymbol{Y} \in R^{m\times m}$ and $\boldsymbol{Z} \in R^{m\times m}$ are all diagonal matrix, $\boldsymbol{\gamma} \ge 0$ and $\boldsymbol{\pi} \ge 0$ can ensure dual feasible, $\boldsymbol{y} \ge 0$ and $\boldsymbol{z} \ge 0$ can ensure primal feasible.

The procedure of the interior point algorithm is an iterative process. From a given initial factor μ^0 and initial point $\boldsymbol{w}^0$, we can solve the non-linear formulation eqn.19 and get step on the corrective direction. After revised vector $\boldsymbol{w}$, we decreased barrier factor μ^k. In each iterative, we can get corrective vectors in the corrective direction. When μ^k is closed to zero the function has reached its optimal and feasible value.

4.2 Solution procedure

The proposed IP method may be summarized as follow:

Step.1: initialization: set μ^0 and $\boldsymbol{w}^0$, $\boldsymbol{w}^0$ must satisfy the positive condition.

Step.2: on the current point, solve eqn.11 and get a corrective direction. In this paper we use Newton-R method to built corrective equations. That is shown in eqn.19, eqn.20 and eqn.21.

Where

$\boldsymbol{\Gamma} = diag(\gamma_1, \gamma_2, \cdots, \gamma_m)$

$\boldsymbol{\Pi} = diag(\pi_1, \pi_2, \cdots, \pi_m)$

$\boldsymbol{I} = diag(1,1,\cdots,1)$.

In this step, we should notice that eqn.19 has already omitted the superscript of iterative counter.

$$\begin{bmatrix} \frac{\partial^2 L_\mu}{\partial \boldsymbol{w}^2} & 0 & 0 & -\left[\frac{\partial \boldsymbol{g}}{\partial \boldsymbol{x}}\right]^{\mathrm{T}} & -\left[\frac{\partial \boldsymbol{h}}{\partial \boldsymbol{x}}\right]^{\mathrm{T}} & \left[\frac{\partial \boldsymbol{h}}{\partial \boldsymbol{x}}\right]^{\mathrm{T}} \\ 0 & \boldsymbol{\Gamma} & 0 & 0 & \boldsymbol{Y} & 0 \\ 0 & 0 & \boldsymbol{\Pi} & 0 & 0 & \boldsymbol{Z} \\ -\left[\frac{\partial \boldsymbol{g}}{\partial \boldsymbol{x}}\right] & 0 & 0 & 0 & 0 & 0 \\ -\left[\frac{\partial \boldsymbol{h}}{\partial \boldsymbol{x}}\right] & \boldsymbol{I} & 0 & 0 & 0 & 0 \\ \left[\frac{\partial \boldsymbol{h}}{\partial \boldsymbol{x}}\right] & 0 & \boldsymbol{I} & 0 & 0 & 0 \end{bmatrix} \begin{bmatrix} \Delta\boldsymbol{x} \\ \Delta\boldsymbol{y} \\ \Delta\boldsymbol{z} \\ \Delta\boldsymbol{\lambda} \\ \Delta\boldsymbol{\gamma} \\ \Delta\boldsymbol{\pi} \end{bmatrix} = \begin{bmatrix} \boldsymbol{b}_x \\ \boldsymbol{b}_y \\ \boldsymbol{b}_z \\ \boldsymbol{b}_\lambda \\ \boldsymbol{b}_\gamma \\ \boldsymbol{b}_\pi \end{bmatrix} \quad (19)$$

$$\left[\frac{\partial^2 L_\mu}{\partial \boldsymbol{x}^2}\right] = \left[\frac{\partial^2 f}{\partial \boldsymbol{x}^2}\right] - \left[\frac{\partial^2 \boldsymbol{g}}{\partial \boldsymbol{x}^2}\right]^{\mathrm{T}} \boldsymbol{\lambda} - \left[\frac{\partial^2 \boldsymbol{h}}{\partial \boldsymbol{x}^2}\right]^{\mathrm{T}} \boldsymbol{\gamma} + \left[\frac{\partial^2 \boldsymbol{h}}{\partial \boldsymbol{x}^2}\right]^{\mathrm{T}} \boldsymbol{\pi} \quad (20)$$

$$\begin{bmatrix} \boldsymbol{b}_x \\ \boldsymbol{b}_y \\ \boldsymbol{b}_z \\ \boldsymbol{b}_\lambda \\ \boldsymbol{b}_\gamma \\ \boldsymbol{b}_\pi \end{bmatrix} = \begin{bmatrix} -\left[\frac{\partial f}{\partial \boldsymbol{x}}\right] + \left[\frac{\partial \boldsymbol{g}}{\partial \boldsymbol{x}}\right]^{\mathrm{T}} \boldsymbol{\lambda} + \left[\frac{\partial \boldsymbol{h}}{\partial \boldsymbol{x}}\right]^{\mathrm{T}} \boldsymbol{\gamma} - \left[\frac{\partial \boldsymbol{h}}{\partial \boldsymbol{x}}\right]^{\mathrm{T}} \boldsymbol{\pi} \\ -\boldsymbol{Y}\boldsymbol{\gamma} + \mu^k \boldsymbol{u} \\ -\boldsymbol{Z}\boldsymbol{\pi} + \mu^k \boldsymbol{u} \\ -\boldsymbol{g}(\boldsymbol{x}) \\ -\boldsymbol{h}(\boldsymbol{x}) + \boldsymbol{y} + \boldsymbol{h}^{\min} \\ \boldsymbol{h}(\boldsymbol{x}) + \boldsymbol{z} - \boldsymbol{h}^{\max} \end{bmatrix} \quad (21)$$

Step.3: on the corrective direction, we revise vector of dual variables and vector of primal variables. That is shown as eqn.22 and eqn.23.

Where β is a scalar quantity $\beta \in [0,\ 1]$, in this paper, to ensure the positive condition we set $\beta = 0.9995$; α_p^k and α_d^k are represented step of dual variable and primal variable respectively, they can be calculated by eqn.24 and eqn.25. δ is represented a given permit error.

$$\begin{bmatrix} \boldsymbol{x} \\ \boldsymbol{y} \\ \boldsymbol{z} \end{bmatrix}^{(k+1)} = \begin{bmatrix} \boldsymbol{x} \\ \boldsymbol{y} \\ \boldsymbol{z} \end{bmatrix}^{(k)} + \beta\alpha_p^k \begin{bmatrix} \Delta\boldsymbol{x} \\ \Delta\boldsymbol{y} \\ \Delta\boldsymbol{z} \end{bmatrix} \quad (22)$$

$$\begin{bmatrix} \boldsymbol{\lambda} \\ \boldsymbol{\gamma} \\ \boldsymbol{\pi} \end{bmatrix}^{(k+1)} = \begin{bmatrix} \boldsymbol{\lambda} \\ \boldsymbol{\gamma} \\ \boldsymbol{\pi} \end{bmatrix}^{(k)} + \beta\alpha_d^k \begin{bmatrix} \Delta\boldsymbol{\lambda} \\ \Delta\boldsymbol{\gamma} \\ \Delta\boldsymbol{\pi} \end{bmatrix} \quad (23)$$

$$\alpha_p^k = \min\left\{1, \min_{\Delta y_i \le -\delta}\left\{\frac{y_i}{\Delta y_i}\right\}, \min_{\Delta z_i \le -\delta}\left\{\frac{z_i}{\Delta z_i}\right\}\right\} \quad (24)$$

$$\alpha_d^k = \min\left\{1, \min_{\Delta \gamma_i \le -\delta}\left\{\frac{\gamma_i}{\Delta \gamma_i}\right\}, \min_{\Delta \pi_i \le -\delta}\left\{\frac{\pi_i}{\Delta \pi_i}\right\}\right\} \quad (25)$$

Step.4: check convergence criteria: The convergence criteria are shown as eqn.26.

$$\begin{cases} \mu^k \le \varepsilon_0 \\ \|\boldsymbol{g}(\boldsymbol{x})\| \le \varepsilon_1 \\ \|\Delta\boldsymbol{x}\| \le \varepsilon_2 \\ \dfrac{\left|f(\boldsymbol{x}^k) - f(\boldsymbol{x}^{k-1})\right|}{\left|f(\boldsymbol{x}^k)\right|} \le \varepsilon_3 \end{cases} \quad (26)$$

On the current point, if the results satisfy the convergence criteria, we will end the iterative process and print out the optimal solution. Otherwise we continue to Step.5.

Step.5: according to eqn.27, we revise the barrier factor and return to Step.2:

$$\mu^{k+1} = \tau^k \frac{(\boldsymbol{y}^k)^{\mathrm{T}}\boldsymbol{\gamma}^k + (\boldsymbol{z}^k)^{\mathrm{T}}\boldsymbol{\pi}^k}{2m} \quad (27)$$

Where $0 < \tau^k < 1.0$, $\tau^k = \max\{0.99\tau^{k-1}, 0.1\}$, $\tau^0 = 0.2 \sim 0.3$ and m is the dimension of vector $\boldsymbol{y}$ or $\boldsymbol{z}$.

5 Case studies

In this section the proposed MOLC model and primal dual IPM are applied to a modified IEEE-30 bus system and an IEEE-118 bus system. The results of load curtailment program are discussed to observe the effect of the proposed MOLC model.

The data (assumed) for the *NC* bus set and the generation available after the contingency (loss of generation) for each of the test systems are given. The curtailable portion is taken in proportion to the original load on the bus i ($i \in NC$). Cost factors of load curtailment are assumed to be monetary unit per MW, respectively, for each bus i ($i \in NC$).

For case studies, the MOLC program and PDIPM program in FORTRAN were employed to analyze test cases.

5.1 The modified IEEE-30 bus system

Fig.1 depicts the IEEE-30 bus system, which is extracted from [17], representing 6 generations and

41 transmission lines. Generation data and load curtailable proportion data are given in Table.6 and Table.1, respectively. The contingency scenario is assumed as loss of generation 3. In this scenario the system is faced with power lines overloaded and power generation inadequacy.

Results for the normal load curtailment program (without the consideration of security margin) are reported in Table.2; the normal load curtailment program value in this table was computed offline using the load and generation data. Table.3, on the other hand, shows the solution obtained for the proposed MOLC for $\omega = 10^{-3}$, since the voltage security margin index of the system is not being really "optimized", with mostly the cost of load curtailment being considered in the objective function. For both solutions, generator voltages are at their maximum limits, as expected, since this condition generally provides lower cost of load curtailments.

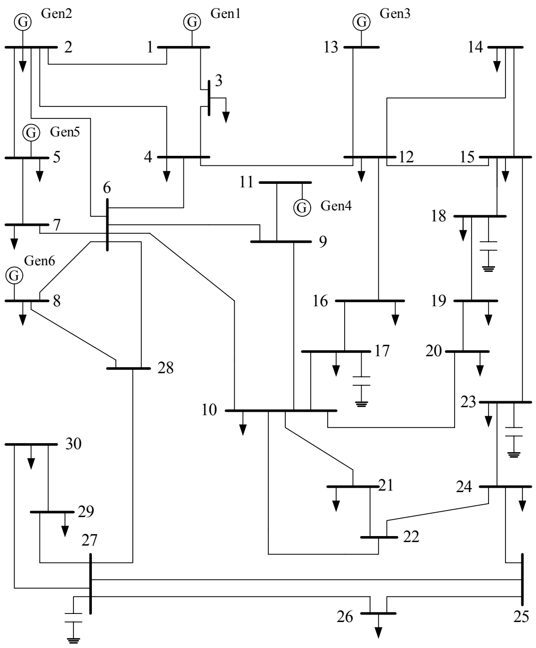

Fig.1. The modified IEEE-30 bus system

Table 1 The data assumed for NC bus set of the modified IEEE 30 bus system

NC Bus No.	Bus-02	Bus-05	Bus-07	Bus-21
P_{Li}(MW)	21.7	94.2	22.8	17.5
$P_{ci}^{\max}$(MW)	10	30	15	10
k_{ci}(M$/MW)	0.2	0.25	0.3	0.35

Table 2 Result of load curtailment of the modified IEEE 30 bus system after contingency

NC bus no.		Bus-02	Bus-05	Bus-07	Bus-21
P_{ci}(MW)	normal	9.5	27.0	9.8	3.9
	ω=10^{-3}	9.4	26.9	9.5	4.4

However, in comparison with the normal load curtailment program, the solution of the proposed method provides better tradeoff between the voltage security margin and cost of load curtailment, which demonstrates that the MOLC results provide a better security level to the system operator, even though the costs of load curtailment are higher.

Fig.2 shows the effect of the weighting factor ω in the total cost level of load curtailment and the minimum voltage security margin. Observe that, as expected, the more the weight, the higher security level, but, at the same time, the higher cost of load curtailment. This is due to the two conflicting objective functions, as ω increases, congestion is minimized (security margin is maximized) by both the reducing f_1 and increasing f_2. Fig.2 depicts the load curtailment of each bus i ($i \in NC$) as ω varies, illustrating the transition from a market problem to a security problem. Observe how the cost of load curtailment increases as the security level increase, since the solution makes a tradeoff between the cost and the security.

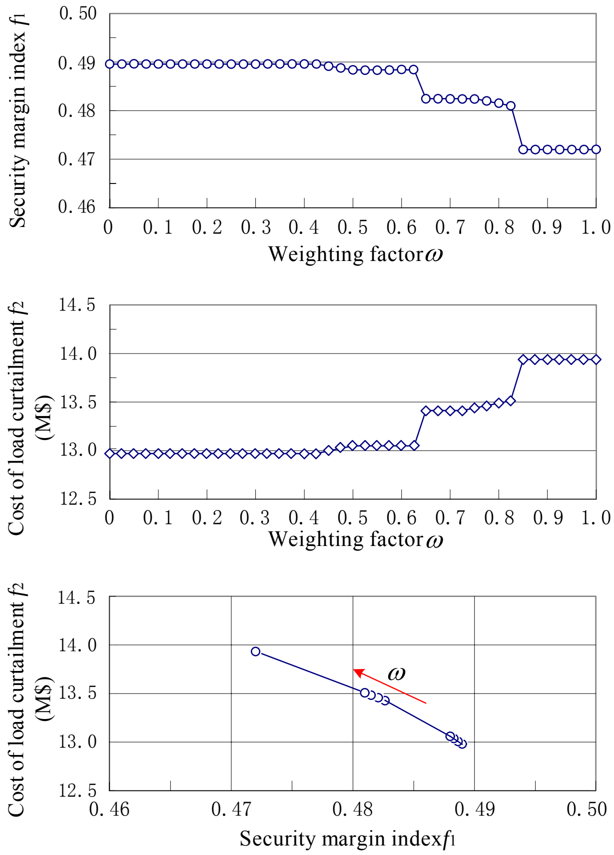

Fig.2 The security margin and cost of load curtailment for the modified IEEE-30 bus system

Furthermore, even though the cost of load curtailment is increase, the security margin level may slightly increase, accordingly to the power dispatch which better matches the obtained security margin. Fig.2 depicts the security margin level as a function of load curtailment with respect to the value of the weighting factor ω, illustrating that the relationship between system security margin level and load curtailment level is not obviously and very much depends on the load curtailment level; in other words, as ω increase (i.e., when system security becomes more significant in the optimization problem), the cost of load curtailment does not show any obvious relationship with respect to the security margin level.

Fig.3 shows the effect of the weighting factor ω in the load curtailment of each bus i ($i \in NC$). Observe that, as expected, he more the weight, the higher security level. But the load curtailment level of each bus i ($i \in NC$) is not obviously and very much depends on the weighting factor ω.

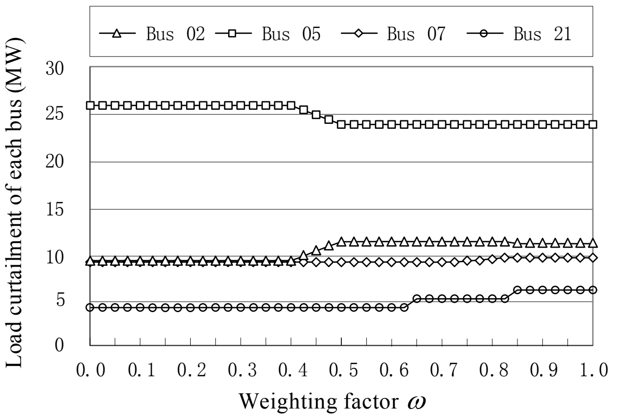

Fig.3 Load curtailment of each bus i ($i \in NC$) of the modified IEEE-30 bus system

5.2 The IEEE-118 bus system

The IEEE-118 bus system can be found in [18]. It has 54 generators and 186 lines. The contingency scenario is assumed as loss of generation 5. In this scenario the system is faced with power lines overloaded and power generation inadequacy.

Results for the normal load curtailment program (without the consideration of security margin) are reported in Table.3; the normal load curtailment program value in this table was computed offline using the load and generation data. Table.4, on the other hand, shows the solution obtained for the proposed MOLC for $\omega = 10^{-3}$, since the voltage security margin index of the system is not being really "optimized", with mostly the cost of load curtailment being considered in the objective function. For both solutions, generator voltages are at their maximum limits, as expected, since this condition generally provides lower cost.

Table 3 The data assumed for *NC* bus set of the modified IEEE-118 bus system

NC Bus No.	Bus-15	Bus-59	Bus-80	Bus-90
P_{Li}(MW)	90	277	130	163
$P_{ci}^{\max}$(MW)	60	200	80	120
k_{ci}(M$/MW)	0.2	0.25	0.3	0.35

Table 4 Result of load curtailment of the modified IEEE-118 bus system after contingency

NC bus no.		Bus-15	Bus-59	Bus-80	Bus-90
P_{ci} (MW)	normal	41.6	166.6	75.8	91.4
	ω=10^{-3}	41.2	164.6	76.1	91.5

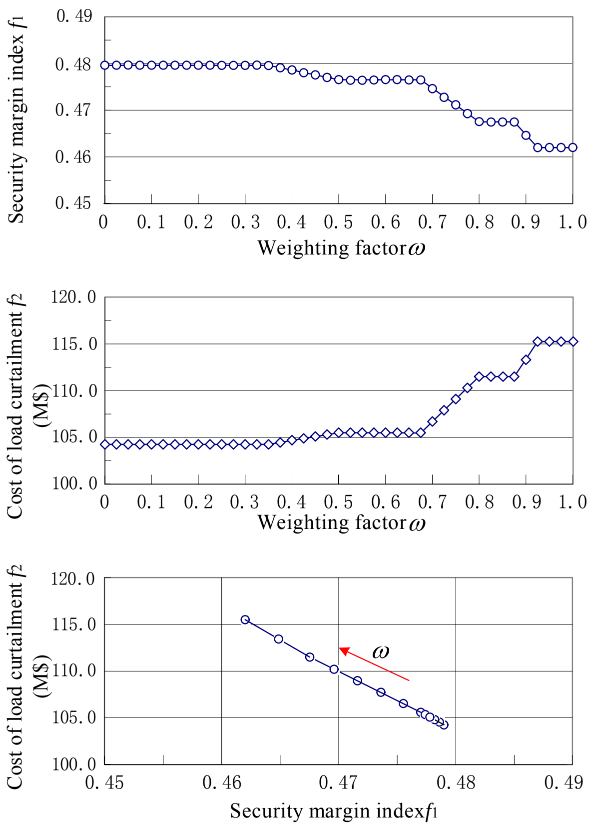

Fig.4 The security margin and cost of load curtailment for the modified IEEE-118 bus system

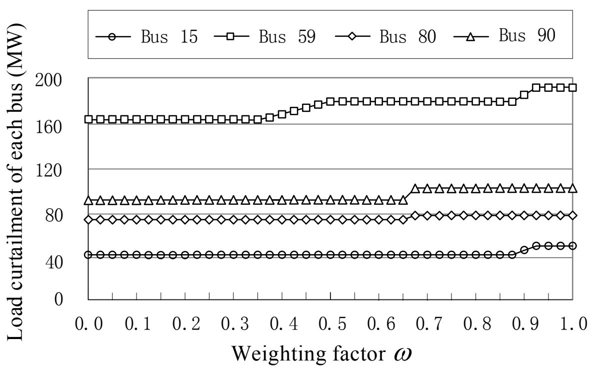

Fig.5 Load curtailment of each bus i ($i \in NC$) of the IEEE-118 bus system

Fig.4 shows the effect of the weighting factor ω in the total cost level of load curtailment level and the minimum voltage security margin. Observe that, as expected, showing a similar behavior as in the case of the modified IEEE-30 bus system.

Fig.5 shows the effect of the weighting factor ω in the load curtailment of each bus i ($i \in NC$). Observe that, the load curtailment level of each bus i ($i \in NC$) is not obviously and very much depends on the weighting factor ω .

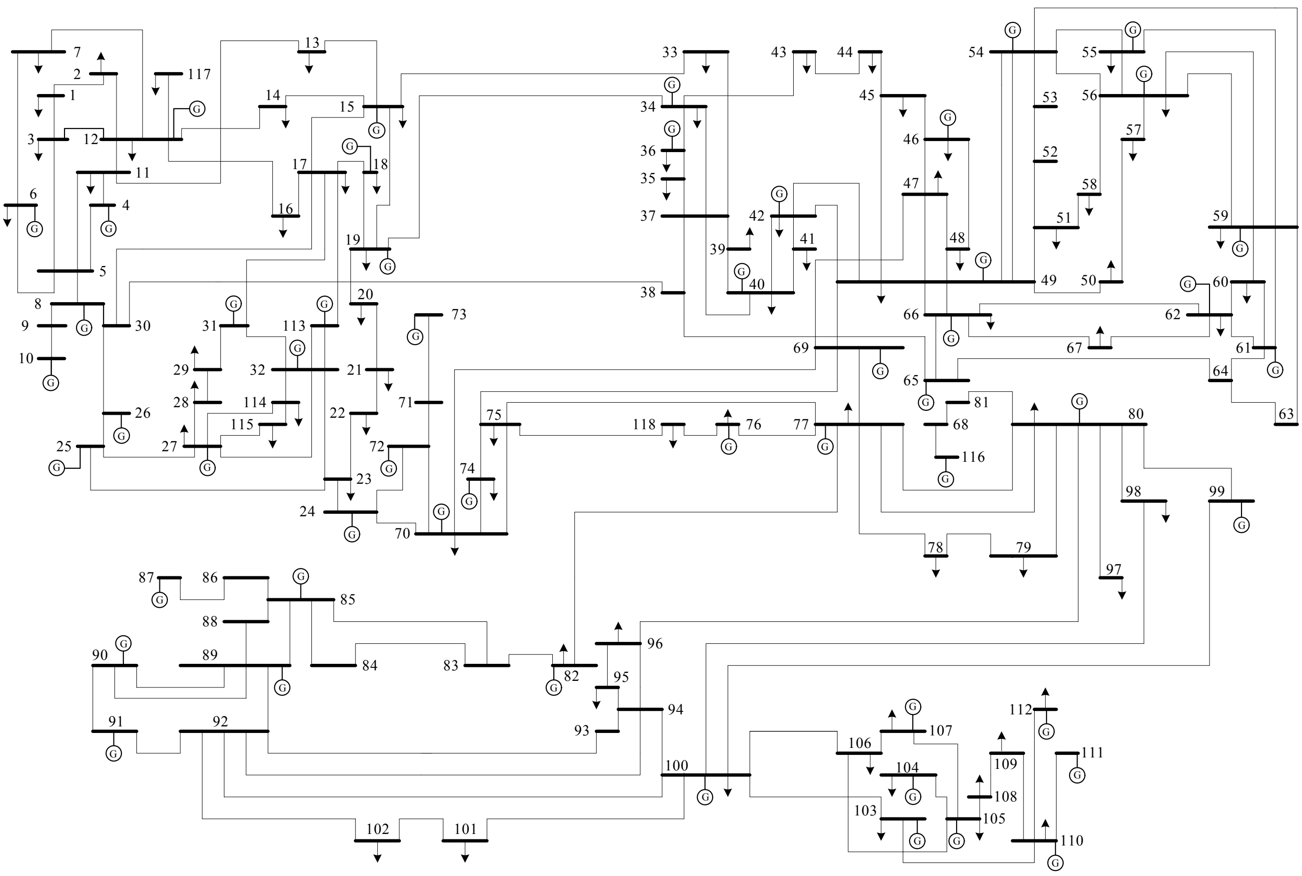

Fig.6 IEEE-118 bus system

6 Conclusion

The phenomenon of congestion is such that it can adversely affect the physical transmission network and the related economic to a significant extent. In this paper a multi-objective load curtailment (MOLC) approach under deregulated environment is presented to deal with this problem and tested on two systems. The result obtained with the proposed technique, shows that proper representation of system security and overall cost of load curtailment.

The results give the tradeoff between the security margin and the cost, which can help the system operator to take the appropriate decision regarding load curtailment. The tradeoff gives the range of secure operation of the system and the corresponding cost involved at different operating points. Therefore, depending upon the base case state of the system, the system operator can curtail loads in order to maximize the overall benefit (in terms of security margin and the cost incurred). Therefore, this methodology provides a way to mitigate congestion.

Acknowledge

For the research presented in this paper the authors gratefully acknowledge the generous financial support provided by Shanghai Key Science and Technology Research Program (no.041612012) and the Scientific Research Foundation for the Returned Overseas Chinese Scholars (no.2005383).

Appendix A: Data of the modified IEEE-30 bus system

Table 5 Bus data for a modified IEEE-30 bus system

Bus no.	P_L [MW]	Q_L [Mvar]	P_G [MW]	Q_G [Mvar]
01 (slack)	0.0	0.0	110	±70
02	21.7	12.7	50	±40
03	2.4	1.2	--	--
04	7.6	1.6	--	--
05	94.2	19.0	30	±20
06	0.0	0.0	--	--
07	22.8	10.9	--	--
08	30.0	30.3	30	±20
09	0.0	0.0	--	--
10	5.8	2.0	--	--
11	0.0	24.0	30	±20
12	11.2	7.5	--	--
13	0.0	24.0	50	±40
14	6.2	1.6	--	--
15	8.2	2.5	--	--
16	3.5	1.8	--	--
17	9.0	5.8	--	--
18	3.2	0.9	--	--
19	9.5	3.4	--	--
20	2.2	0.7	--	--
21	17.5	11.2	--	--
22	0.0	0.0	--	--
23	3.2	1.6	--	--
24	8.7	6.7	--	--
25	0.0	0.0	--	--
26	3.5	2.3	--	--
27	0.0	0.0	--	--
28	0.0	0.0	--	--
29	2.4	0.9	--	--
30	10.6	1.9	--	--

Table 6 Line data for a modified IEEE-30 bus system

Line i-j	R_{ij} [p.u.]	X_{ij} [p.u.]	$B_i/2$ [p.u.]	$T_{\max}$ [MVA]
01-02	0.0192	0.0575	0.0264	100
01-03	0.0452	0.1852	0.0204	45
02-04	0.0570	0.1737	0.0184	40
03-04	0.0132	0.0379	0.0042	40
02-05	0.0472	0.1983	0.0209	80
02-06	0.0581	0.1763	0.0187	50
04-06	0.0119	0.0414	0.0045	40
05-07	0.0460	0.1160	0.0102	40
06-07	0.0267	0.0820	0.0085	40
06-08	0.0120	0.0420	0.0045	40
09-11	0.0000	0.2080	0.0000	50
09-10	0.0000	0.1100	0.0000	40
12-13	0.0000	0.1400	0.0000	60
12-14	0.1231	0.2559	0.0000	40
12-15	0.0662	0.1304	0.0000	30
12-16	0.0945	0.1987	0.0000	30
14-15	0.2210	0.1997	0.0000	30
16-17	0.0524	0.1923	0.0000	30
15-18	0.1073	0.2185	0.0000	30
18-19	0.0639	0.1292	0.0000	30
19-20	0.0340	0.0680	0.0000	30
10-20	0.0936	0.2090	0.0000	30
10-17	0.0324	0.0845	0.0000	30
10-21	0.0348	0.0749	0.0000	30
10-22	0.0727	0.1499	0.0000	30
21-22	0.0116	0.0236	0.0000	30
15-23	0.1000	0.2020	0.0000	30
22-24	0.1150	0.1790	0.0000	30
23-24	0.1320	0.2700	0.0000	30
24-25	0.1885	0.3292	0.0000	30
25-26	0.2544	0.3800	0.0000	30
25-27	0.1093	0.2087	0.0000	30
27-29	0.2198	0.4153	0.0000	30
27-30	0.3202	0.6027	0.0000	30
29-30	0.2399	0.4533	0.0000	30
08-28	0.0636	0.2000	0.0214	30
06-28	0.0169	0.0599	0.0065	30
09-06	0.0000	0.2080	0.0000	30
10-06	0.0000	0.5560	0.0000	30
12-04	0.0000	0.2560	0.0000	30
27-28	0.0000	0.3960	0.0000	30

Appendix B: List of Symbols

Table 7 List of symbols

N	: Bus set of all bus
NG	: Bus set of generations
NC	: Bus set of load curtailments
L	: Set of transmission lines
$\boldsymbol{f}(\cdot)$	: Vector of objective functions
$\boldsymbol{g}(\cdot)$	: Vector of power flow equations
$\boldsymbol{h}(\cdot)$	: Vector of in-equations
$\boldsymbol{h}^{\min}$	: Lower limitation of inequality constraints
$\boldsymbol{h}^{\max}$	: Upper limitation of inequality constraints
$\boldsymbol{x}$	: Vector of decision variables
$\boldsymbol{V}$	: Vector of bus voltages
$\boldsymbol{\theta}$	: Vector of bus phase angles
$\boldsymbol{P}_c$	: Vector of real load curtailments
λ	: Security margin of the system
k_i	: Cost factor of load curtailment at bus i
P_{ci}	: Real load curtailment of bus i

Q_{ci}	: Reactive load curtailment of bus i
$P_i(\cdot)$	: Real power injection at bus i
$Q_i(\cdot)$	: Reactive power injection at bus i
P_{Li}	: Real power at load bus i
Q_{Li}	: Reactive power at load bus i
P_{Gi}	: Real power generation at bus i
$P_{Gi}^{\min}$	: Minimum real power generation at generation bus i
$P_{Gi}^{\max}$	: Maximum real power generation at generation bus i
Q_{Gi}	: Reactive power generation at bus i
$Q_{Gi}^{\min}$	: Minimum reactive power generation at generation bus i
$Q_{Gi}^{\max}$	: Maximum reactive power generation at generation bus i
$T_l(\cdot)$	: Power flow of line l
$T_l^{\max}$	: Power flow limitation of line l
V_i	: Voltage magnitude at bus i
$V_i^{\min}$	: Voltage lower limit constraint at bus i
$V_i^{\max}$	: Voltage upper limit constraint at bus i
ϕ_i	: Power factor angle of load bus i
Z_i^{Load}	: Load impedance of bus i
Z_{ii}^{Bus}	: Self-impedance of bus i

References:

[1] Bhattacharya Kankar, Bollen Math H.J., Daalder Jaap E. Operation of Restructured Power Systems [M]. 1st ed, Kluwer Academic Publishers. Boston, MA. 2001.

[2] W.S. Read, W.K. Newman. I.J. Perez-Arriaga, H Rudnick. M.R. Gent, and A. J. Roman. Reliability in the new market structure (part 1), *IEEE Power Eng. Rev*. Vol.19, no.12, 1999, pp. 4-5.

[3] Fang R.S, David A.K. Transmission congestion management in an electricity market [J]. *IEEE Transactions on Power Systems*, Vol. 14 No.3, 1999, pp. 877-883.

[4] D. Shirmohammadi, B. Wollenberg, A Vojdani. P. Sandrin. Pereira, F. Rahimi, T. Schneider, B. Stott, Transmission dispatch and congestion management in the emerging energy market structures [J], *IEEE Trans. Power Systems*, Vol.13, No.4, 1998, pp. 1466-1474.

[5] J. Kehler, Procuring load curtailment for grid security to Alberta [C], *Proceedings of the IEEE PES Winter Meeting 2001*, Columbus, 2001, pp. 234-235,.

[6] A Lossi, Trade curtailment schemes for the security control of the transmission network in a deregulated environment [J]. *Electrical Power Energy Systems*, Vol.24, 2002, pp. 9-17.

[7] Durgesh P. Manjure, Elham B. Makram. Optimal load curtailment as a bi-criteria program [J]. *Electric Power Systems Research*, Vol.66, 2003, pp. 155-161.

[8] Huang, G.M., Nair, N.-K.C. Voltage stability constrained load curtailment procedure to evaluate power system reliability measures [C]. *IEEE Power Engineering Society Winter Meeting*, 2002. Vol.2, pp. 761-765.

[9] A.M. Chebbo, M.R. Irving, M.J.H. Sterling, Voltage collapse proximity indicator behaviour and implications [J]. *IEE Proceeding Generation Transmission Distribution*, Vol.193, No.3, 1992, pp. 241-252.

[10] P.Kessel. And H.Glavitch. Estimating the voltage stability of a power system [J]. *IEEE Trans on Power Deliver*, Vol. PWRD-1, No.3, 1986, pp. 346-354.

[11] Wu Yuchi, Atif. S. Debs, Roy E Marsten. A direct nonlinear predictor corrector primal-dual interior point algorithm for optimal power flow [J]. *IEEE Trans on Power Systems*, Vol.9, No.2, 1994, pp. 876-883.

[12] Quintana VH, Torres GL, Medina-Palomo J. Interior-point methods and their applications to power systems: a classification of publications and software codes [J]. *IEEE Trans Power Systems*, Vol.15, No.1, 2000, pp. 170-176.

[13] H. Wei, H.Sasaki and R. Yokoyama. An application of interior point quadratic programming algorithm to power system optimization problem [J]. *IEEE Trans on Power Systems*, Vol.11, No.1, 1996, pp. 260-267.

[14] H. Wei, H.Sasaki and J.Kubokawa. An interior point nonlinear programming for optimal power flow problem with a novel data structure [J]. *IEEE Trans on Power Systems*, Vol.13, No.3.1998, pp.

[15] S. Granville. Optimal reactive dispatch through interior point methods [J]. *IEEE Trans on Power Systems*, Vol.9, No.1, 1994, pp. 136-146.

[16] James A Momoh, M E E Hawary, Ramababu Adapa. A review of selected optimal power flow literature to 1993 Part II: Newton, Linear Programming and Interior Point Methods [J]. *IEEE Trans on Power Systems*, Vol.14, No.1, 1999, pp. 105-111.

[17] Vlaisavljevic, Djukanovic, Sobajic, Babic. Fuzzy linear programming based optimal power system rescheduling including preventive re-dispatch. *IEEE Transaction on*

Power Systems, Vol.14, No.2, 1999, pp. 525-531.

[18] University of Washington, Power systems Test Case Archive. http//:www.ee.washingtong.edu /research/pstca/.

SIGE LIU was born in Jilin Province, China on November 15, 1975. He received the B.S. degree and the M.S. degree in electric power engineering from Northeast Dianli University in 1998 and 2004. Now, He is currently pursuing his PH.D degree in Shanghai Jiao Tong University (SJTU), Shanghai, China. His special fields of interest included power system planning, analysis, and etc.

XIAOXIN ZHOU was born in Shandong Province, China, on April 7, 1940. He Graduated from Electrical Engineering Department of Tsinghua University in 1965. He is an academician of Chinese Academy of Sciences since 1993. His special field includes power system planning, operation and automation, nuclear power station modeling and system simulation, FACTS technology, power grids interconnection etc. He is a fellow of IEEE.

MINGTIAN FAN was born in Huan Province, China on December 8, 1954. She received the B.S. degree in South China University of Technology, the M.S. degree in CEPRI and the P.H.D degree in Tsinghua University. Her special fields of interest included power system planning, analysis, and etc.

HAOZHONG CHENG was born in Zhejiang Province, China. He receive his BSc, MSc and PHD degrees in Department of Electrical Engineering at Shanghai Jiaotong University, and is now a professor of Shanghai Jiaogtong University. His research interests cover power system planning, voltage stability, power quality and electricity market.